DESIGN SYNTHESIS AND EVALUATION OF MULTI TARGATED THERAPEUTICS ON ALZHEIMER'S DISEASE

Lavdeep Singh

Research Scholar, Kharvel Subharti College of Pharmacy, Swami Vivekanand Subharti University, Meerut, Uttar Pradesh, India

Vikrant Verma

Department of Pharmaceutical Chemistry, Kharvel Subharti College of Pharmacy, Swami Vivekanand Subharti University, Meerut, Uttar Pradesh, India

Ganesh Prasad Mishra

Department of Pharmaceutical Chemistry, Kharvel Subharti College of Pharmacy, Swami Vivekanand Subharti University, Meerut, Uttar Pradesh, India

Prabhash Nath Tripathi

Department of Pharmaceutical Technology, Meerut Institute of Engineering and Technology, NH-58, Baghpat Bypass Road, Meerut, India

*Corresponding Author: Vikrant Verma

*Department of Pharmaceutical Chemistry, Kharvel Subharti College of Pharmacy, Swami Vivekanand Subharti university, Meerut, Uttar Pradesh, India,

Email: vijeetsingh84@rediffmail.com

Abstract:

The multitarget-coordinated methodology offers a viable and promising worldview to treat neurodegenerative disease, like Alzheimer's disease. in this, a progression of N-(4-(benzo[d]thiazol analogs (3a-3g) were planned and synthesized as multi-useful inhibitors of acetylcholinesterase (ACHE) with moderate to Significant inhibitory results. Bta3d was the tested inhibitor with the greatest and most balanced inhibition of targets. Compounds are likewise tried with scopolamine induced rat model and y maze tests. Ex vivo and biochemical investigation for ex vivo studies and Histopathology of the compound. further, acetyl choline esterase inhibition was seen by compound BTA 3d in the y maze task and different ex vivo, in vivo. In vitro studies with molecular docking study.

Keywords; acetylcholine esterase (ACHE), Alzheimer's disease, histopathology, Y-maze, ex vivo, in vivo, BTA (benzothiazole), Molecular docking.

INTRODUCTION

Alzheimer's disease (AD) is disturbing neuro progressive sickness, causes shortages in memory, and behaviour. Numerous speculations have been planned for the handling of Alzheimer's, with hindrance of cholinesterase, restraint of amyloid protein development, and restraint of tau protein aggregation. Cholinergic hypothesis is known to assume a basic part in mental presentation and cholinergic hypothesis has been seen to vanish in Alzheimer's step by step**. (1)** For this reason, a treatment line has been laid out to treat side effects utilizing cholinesterase inhibitors. A few FDA-supported opponent of Alzheimer's medicates presently accessible clinically (like cholinesterase inhibitors: donepezil, rivastigmine, galantamine) give just incomplete alleviation of side effects and can't stop or opposite illness movement. Donepezil works in Alzheimer's sickness Specically as an acetylcholinesterase inhibitor at gentle to direct levels. Nonetheless, donepezil has aftereffects like queasiness, loose bowels, shortcoming, dazedness, urinary incontinence, and a sleeping disorder. **(2).** Since considering the age of the patient gathering, the utilization of a solitary specialist that represses every one of them rather than independent specialists will likewise work with. It has been accounted for that benzothiazole ring gives every one of the three of these impacts (**3**). In this manner, it was picked as a pharmacophore in the principal construction of our mixtures. Not with standing the previously mentioned properties of benzothiazole ring, it likewise has use as a neuroprotective and amyloid-repressing specialist. The fexibility provided by these groups in the chemical structure helps ensure proper binding to the enzyme active site's valley. Inside the extent of this review, the mixtures were intended to be comparative long to donepezil and to restrict to the protein dynamic site. In the radiance of this data, both benzothiazole (as an optional amine subsidiaries) was utilized in the design of the objective mixtures. **(4)**

In current research, An original series of mixtures were planned and blended. The biochemical estimation, scopolamine-induced amnesia model, and behavioral activity of the synthesized compounds, as well as their potential in vitro against AChE, were all evaluated. The results of in vitro study were additionally authenticated utilizing in vitro, ex vivo and in Vivo **(5).**

Designing Considerations;

In this experimental work, the synthesized benzothiazole (Bta1, Bta2, Bta3) the primary compound BTA 3d is a part of N-(4-(benzo [d] thiazol-2-yl) phenyl) Hydrazine carboxamide (BTA 3) and its subordinate 3D for their potential opponent of Alzheimer's and perception improving properties with acetylcholine esterase hindrance. BTA 3d analysed by scopolamine induced amnesia model. **(6)**

The benzothiazoles and benzothiazoles 3D shows the acetylcholine esterase inhibitor.

RESULT AND. DISCUSSION

Chemistry:

The Aim of the study to find unique component those synthesis novel molecules with the same chemical structure as benzothiazole. In order to do this, 8 novel compounds were synthesized. a four-step reaction was used to produce the target chemicals. Scheme 1 describes the chemicals' production route. Initially.
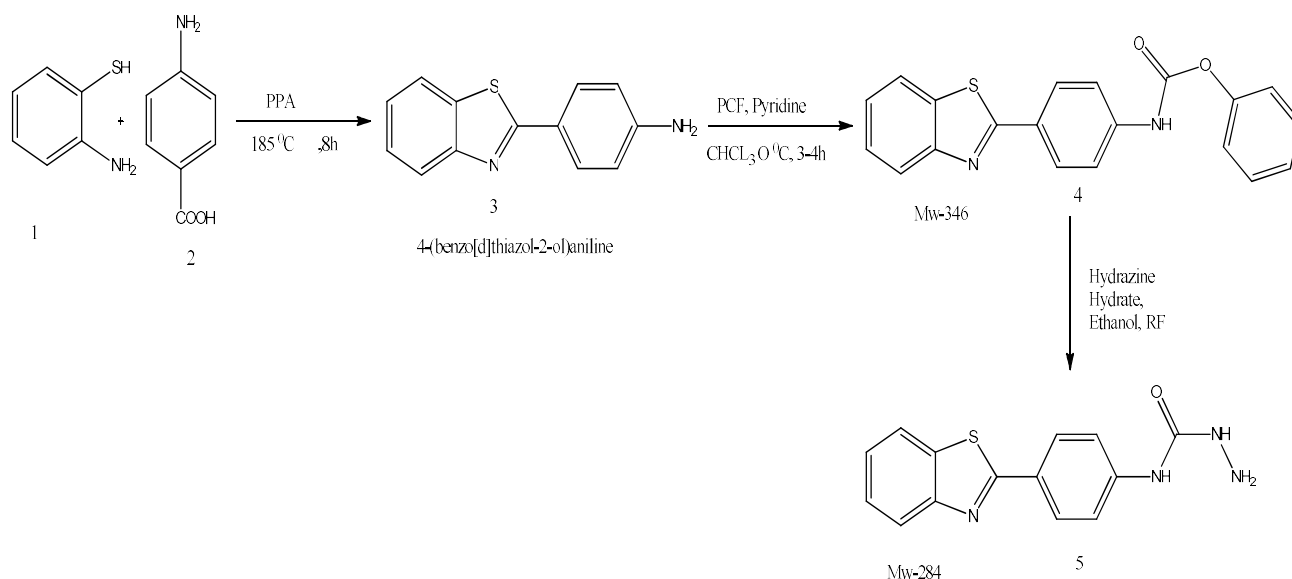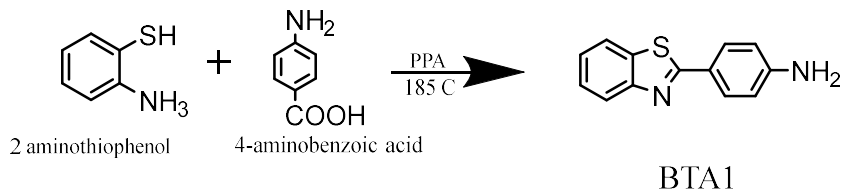
Scheme 1

EXPERIMENTAL

Chemicals and instrumentation

Each and every reagent was attainable financially and purchased from Sigma Aldrich. Slender layer chromatography was used Using silica gel plates with precoating60-F254 to resolve the Rf values once the response advancements were seen (Merck, Germany). The dissolving focuses on a Perfit (India) softening point apparatus were determined using open, thin cylinders with a fixed one end and were recorded as uncorrected. Shimazdu 8400s were used to capture FT-IR spectra, which were then shown as wavenumber Versus percent transmittance. Both the 1H NMR (400 MHz) and the 13C NMR (100 MHz) were recorded on a joyful Analytical (avneo400NB-5054750-jubliant GN greater Noida TMS is used as the internal standard in a spectrophotometer at room temperature**. (7)**

Synthetic scheme:

A. 2-aminothiophenol (1 eq), and PABA (p-amino benzoic acid) are mixed together with solvent polyphosphoric acid (70g) at this chemical mixture reflux at temperature 185°C with the medium speed of magnetic stirrer**. (8)** After 1 hr the reaction mixture colour changes to greenish colour. And the observations of reaction taken on time to time by odour, colour and chemical changes that is observed by thin layer chromatography. reaction takes around 24 hrs for completion after that the magnetic off and take the Rbf at a Seprate place. **(9)**
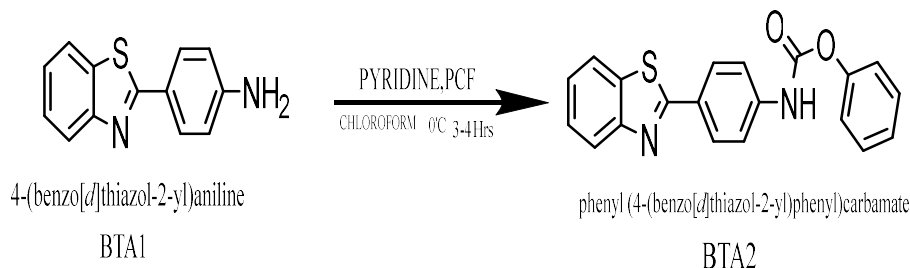
Scheme 2.

Analysis: Yield: 87%. FT-IR (ν, cm–1): 3109 (—NH stretching), 1720 (C=O stretching). 1H NMR (DMSO-d6, ppm): δ 8.03 (2H, aromatic CH), 8.18 (d2H, aromatic CH), 6.58 (2H, aromatic CH), 7.74-6.58 (m, 3H, aromatic CH), 5. (s, 1H, —NH2). 13C NMR (DMSO-d6, ppm): 169.0, 133.2, 152.3, 145.6, 121.8, 121.6, 121.0, 115.1, 129.6, 115.1, 124.5, 124.5, 125.3. Anal. calc. (%) for $C_{13}H_{10}N_2S$; C, 69.00; H, 4.45; N, 12.38, S 14.17.

B. Basic steps for the synthesis of Phenyl(4-benzo[*d*]thiazol-2-yl) phenyl) carbamate
When 4-(benzo(d)thiazol-2-yl) anillin completely dried we follow step 2 reaction with the solvent chloroform wait until step 1 product mixes completely then we have to use ice bath for 0Oc temp. and a medium stirring of solution then pyridine (2 eq.) added drop wise in reaction mixture. After the complete addition of pyridine. Wait 5 mins and add phenyl chloroformate (2.3eq) in reaction mixture. And continue the stirring for 6 hrs at room temperature. And wait until the compound spots clarify TLC.**(10)**
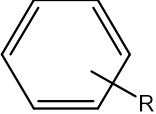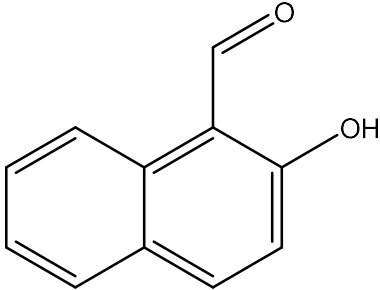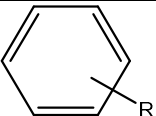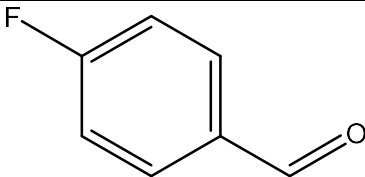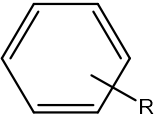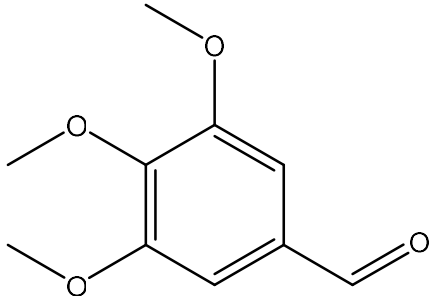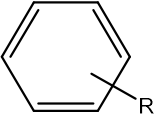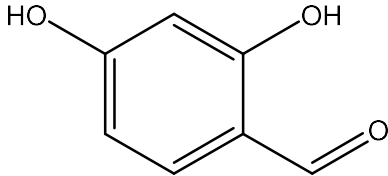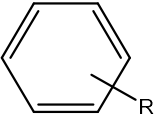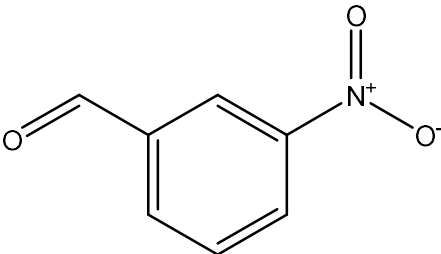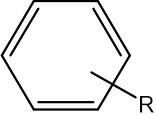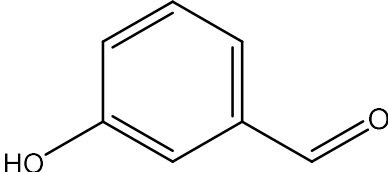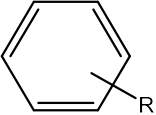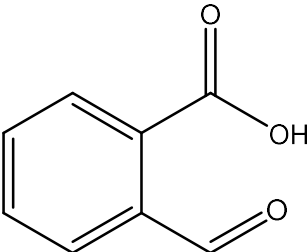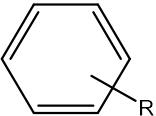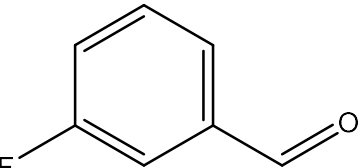

Scheme 3
Analysis: Yield:95 %, FT-IR (ν, cm–1): 3332 (—NH, stretching), 1720 (C=O stretching). 1H NMR (DMSO-d6, ppm): δ 8.02 (d, J = 8.12 Hz, 2H, aromatic CH), 8.18 (d, J = 7.0 Hz, 2H, aromatic CH), 7.23 (t, J = 6.8 Hz, 2H, aromatic CH), 7.98-.23 (m, 3H, aromatic CH), 7. (s, 1H, —NH2). 13C NMR (DMSO-d6, ppm): 169.0, 133.2, 154.4,151.3, 138.0, 121.8, 121.6, 126.6, 121.6, 119.1, 129.5, 121.5, 129.3. Analytical Calculations (%) for $C_{20}H_{14}N_2O_2S$.= C 69.35, H=4.07, N 8.09, O 9.24, S9.26

C. General method for synthesis of N-(4-(benzo[d]thiazol-2-yl) phenyl) Hydrazine carboxamide:
After the complete drying of Phenyl(4-benzo[*d*]thiazol-2-yl) phenyl) carbamate next step reaction with hydrazine hydrate (5 eq.) **(11)** used as reagent and ethanol also used as a solvent. this reaction also a reflux reaction. this reaction also a reflux reaction at 75°C for 4-6 hrs.

phenyl (4-(benzo[*d*]thiazol-2-yl)phenyl)carbamate   *N*-(4-(benzo[*d*]thiazol-2-yl)phenyl)hydrazinecarboxamide

BTA2   BTA3

Scheme 4

Analysis:

Yield:67%, FT-Ir, (*v*, cm–1): 3332 (—NH stretching), 1720 (C=O stretching). 1H NMR (DMSO-d6, ppm): δ 8.02 (d, J = 8.12 Hz, 2H, aromatic CH), 8.18-7.53 (d, J = 7.0 Hz, 2H, aromatic CH), 4.35(amine) 13C NMR (DMSO-d6, ppm): 169.0, 133.8, 154.4,139.3, 121.4, 121.6, 119.7, 129.0, 121.6, 119-129.5. Anal. calc. (%) for $C_{14}H_{12}N_4OS$; C, 59.14; H, 4.25; N19.70, S11.28.

Derivatives: -

The general method for making derivatives consisted of mixing equal amounts of different aldehydes (1-8), together with the crystallized product BTA3 and refluxing them with ethanol for three to five hours. After the reaction product were cooled and washed with ethanol and recrystallized with ethanol for a pure benzothiazoles derivative.

Note: The R is also used for representing the benzaldehyde attaching group for synthesis of derivatives

GROUP (R)	BENZALDEHYDE

R (benzene ring)	2-HYDROXY-1-NAPHTHALDEHYDE
R (benzene ring)	4 FLUOROBENZALDEHYDE
R (benzene ring)	3,4,5,TRIMETHOXYBENZALDEHYDE
R (benzene ring)	2,4 DIHYDROXYBENZALDEHYDE
R (benzene ring)	3-NITROBENZALDEHYDE

R	![3-hydroxybenzaldehyde structure] **3-HYDROXYBENZALDEHYDE**
R	![2-carboxybenzaldehyde structure] **2-CARBOXYBENZALDEHYDE**
R	![3-fluorobenzaldehyde structure] **3-FLUOROBENZALDEHYDE**

Table.1. Different substituents for synthesis of benzothiazole derivatives

1. N-(4-(benzo[d]thiazol-2-yl)phenyl)-2-((2-hydroxynapthelen-1yl)methylene)Hydrazine-1-carboxamide (3A) (12)
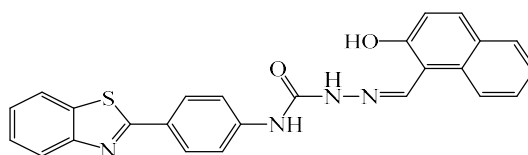
Molecular Formula: C$_{25}$H$_{18}$N$_4$O$_2$S

Molecular Weight: 438.12

Physical state: Solid

Colour: Faint to light greenish crystalline powder

Melting Point: 250-255 °C (Merck and Co., Inc., 2006).

Water Solubility: In water, DMSO,

TLC: (DCM/Methanol 95:05 v/v) and EA/Hexane 20:80 v/v)

Analysis

Yield: 60.0%. FT-IR (ν, cm–1): 3191 (—NH stretching). 1H NMR (DMSO-d6, ppm): δ 12.74 (s, 1H, —OH), 8.90-6.0 (m, aromatic NH), 7.80-8.55 (m, aromatic CH), 7.10–6.82 (m, 3H, aromatic

CH). 13C NMR (DMSO-d6, ppm): 169.0, 132.1, 154.2, 171.2, 139.1, 121.3, 121.9, 126.6, 11.2. Anal. calc. (%) for C25H18N4O2S; C, 68.48; H, 4.14; N, 12.78;S 7.31.

2. N-(4-(benzo[d]thiazol-2-yl)phenyl)-2-((4-fluorobenzylidene)Hydrazine-1-carboxamide (3B) (13)

Chemical properties:
Molecular Formula: C₂₁H₁₅FN₄OS
Molecular Weight: 390.44
Physical state: Solid
Colour: Faint to light yellow crystalline powder
Melting Point: 240-255 °C (Merck and Co., Inc., 2006).
Water Solubility: In water, DMSO,
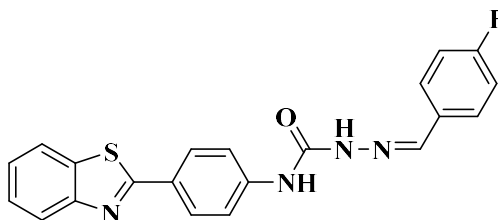**TLC:** (DCM/Methanol 95:05 v/v) and EA/Hexane 20:80 v/v)

Analysis
Yield:65% FT-IR (ν, cm–1): 3494 (—NH stretching). 1H NMR (DMSO-d6, ppm): δ 8.90 (1H, —NH), 7.32-8.55 (m, 2H, aromatic CH), 7.32–7.99 (m, 3H, aromatic CH), (. 13C NMR (DMSO-d6, ppm): 163.0, 150.1, 144.3, 165.4,141.8, 132.6,129.3,115. Anal. calc. (%) for C₂₁H₁₅FN₄0S ; C, 64.60 ; H, 3.87; N, 14.35,F 4.87,0 4.10, S 8.21.

3. *N-(4-(benzo[d]thiazol-2-yl)phenyl)-2-((3,4,5-trimethoxybenzylidene))Hydrazine-1-carboxamide* (3c) (14)

Chemical Properties:
Molecular Formula: C₂₄H₂₂N₄O₄S
Molecular Weight: 462.52
Physical state: Solid
Colour: light red crystalline powder
Melting Point: 180-195 °C (Merck and Co., Inc., 2006).

Water Solubility: In water, DMSO

TLC: (DCM/Methanol 95:05 v/v) and EA/Hexane 20:80 v/v)

Yield: 60%.

Elemental analysis- C 62.32; H-4.79; N-12.11;O,13.84;S 6.93

4. *N-(4-(benzo[d]thiazol-2-yl)phenyl)-2-((2,4-dihydroxybenzylidene)Hydrazine-1-carboxamide* (15)(3D)

Name: N-(4-(benzo[d]thiazol-2-yl) phenyl)-2-((2,4-dihydroxybenzylidene) Hydrazine-1-carboxamide

Molecular Formula: C$_{21}$H$_{16}$N$_4$O$_3$S

Molecular Weight: 404.09

Physical state: Solid

Colour: Faint to light brown crystalline powder
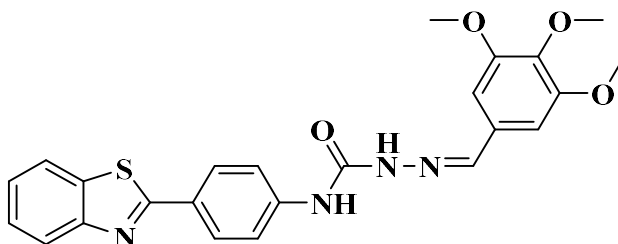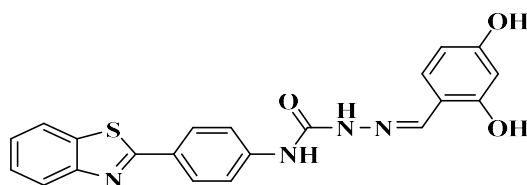
Melting Point: 271-285 °C (Merck and Co., Inc., 2006).

Water Solubility: In low solubility in water, DMSO

TLC: (DCM/Methanol 95:05 v/v) and EA/Hexane 20:80 v/v)

ANALYSIS: - Yield: 58.0%. FT-IR 1704 and 3401 (stretching group). 1H NMR (DMSO-d6, ppm): δ 10.10 (s, 1H, —OH), 8.90 (m, aromatic NH), 8.18 (m, aromatic CH), 7.53–7.99 (m, 3H, aromatic CH). 13C NMR (DMSO-d6, ppm): 163.0, 143.1, 151.2, 161.2, 141.1, 132.3, 111.0, 103.7.6, 11.2.

Elemental analysis – C-62.32, H-3.99, N-13.85; O- 11.87, S7.93,

5. *N-(4-(benzo[d]thiazol-2-yl)phenyl)-2-((3-nitrobenzylidene)Hydrazine-1-carboxamide* (3E) (16)

Chemical properties:

Name: N-(4-(benzo[d]thiazol-2-yl)phenyl)-2-((3-nitrobenzylidene)Hydrazine-1-carboxamide

Molecular Formula: C$_{21}$H$_{15}$N$_5$O$_3$S

Molecular Weight: 417.44

Physical state: Solid

Colour: white crystalline powder

Melting Point: 180-195 °C (Merck and Co., Inc., 2006).

Water Solubility: In water, DMSO,

TLC: (DCM/Methanol 95:05 v/v) and EA/Hexane 20:80 v/v)

6. *N-(4-(benzo[d]thiazol-2-yl)phenyl)-2-((3-hydroxybenzylidene)methylene)*   *Hydrazine-1-carboxamide* **(3F) (17)**

Name: N-(4-(benzo[d]thiazol-2-yl)phenyl)-2-((3-hydroxybenzylidene)methylene) Hydrazine-1-carboxamide

Molecular Formula: $C_{21}H_{16}N_4O_2S$

Molecular Weight: 388.10

Physical state: solid

Colour: Faint to light yellow crystalline
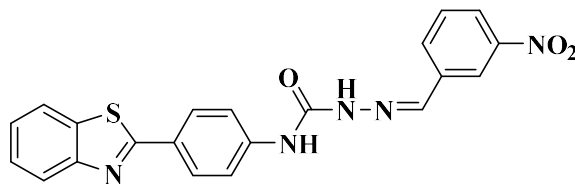
Melting Point: 180-195 °C (Merck and Co., Inc., 2006).

Water Solubility: In water, DMSO,

TLC: (DCM/Methanol 95:05 v/v) and EA/Hexane 20:80 v/v)

Elemental Analysis – C 64.93; H 4.15; N 14.42; O,8.24; S 8.25

7. *2-((2-((4-(benzo[d]thiazol-2-yl)phenyl)carbamoyl)hydrazono)methyl)benzoicacid (3G)(18)*

Name: 2-((2-((4-(benzo[d]thiazol-2-yl) phenyl) carbamoyl) hydrazono) methyl) benzoic acid

Molecular Formula: $C_{22}H_{16}N_4O_3S$

Molecular Weight: 416.09

Physical state: Solid

Colour: light black crystals

Melting Point: 280-295 °C (Merck and Co., Inc., 2006).

Water Solubility: In water, DMSO,

TLC: (DCM/Methanol 95:05 v/v) and EA/Hexane 20:80 v/v)

Elemental analysis- C 63.45, H 3.87; N 13.45; O 11.53; S 7.70

8. *N-(4-(benzo[d]thiazol-2-yl)phenyl)-2-((3-flurobenzylidene)Hydrazine-1-carboxamide* (3H) (19)

Name: *N-(4-(benzo[d]thiazol-2-yl)phenyl)-2-((3-flurobenzylidene)Hydrazine-1-carboxamide*

Molecular Formula: $C_{21}H_{15}FN_4OS$

Molecular Weight: 390.10

Physical state: Solid

Colour: Faint to light orange crystalline powder
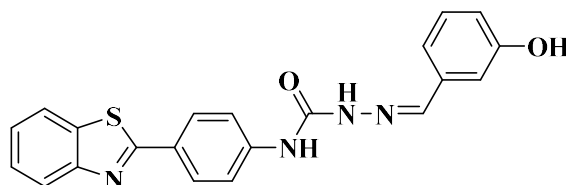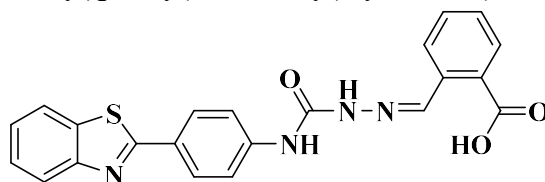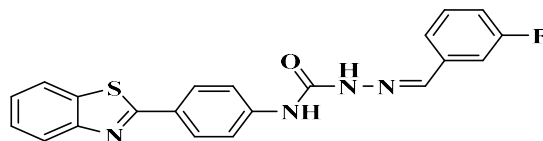
Melting Point: 260°C (Merck and Co., Inc., 2006).

Water Solubility: In water, DMSO,

TLC: (DCM/Methanol 95:05 v/v) and EA/Hexane 20:80 v/v)

Elemental Analysis – C 64.60; H 3.87; F4.87; N 14.35; O,4.10; S 8.21

PHARMACOLOGICAL STUDIES

In vivo studies

Animal

The present experimental study utilized female Wistar rats with a weight range of 180- 250 g, which were obtained from Disease-Free Small Animal House LUVAS Hisar, Haryana1669/GO/ReBiBt-S/Re-L/12/CPCSEA. The animals were housed in hygienic cages located in a temperature-controlled animal facility with an ambient temperature range of 25°C to 3°C relative humidity, and were provided with free access of food and water. (**20**) The behavioural tests were conducted between 9:00 and 17:00. To ensure compliance withheethical standards, the Institutional Animal Ethics Committee IAEC/MIET/2023/089 approved the experimental protocol, which was carried out at the reputable animal house of the Meerut Institute of Engineering and Technology (miet) in Uttar Pradesh, India. Age-matched animals were employed in all experiments to Minimized variance in the experimental groups. (**21**)

Acute Oral Toxicity:

According to the OECD 423 guidelines, the compound BTA 3D caused acute oral toxicity in healthy wister rats (200-210 gm). Tremors, salivation, diarrhoea, lacrimation, sleep, and feeding behavior were among the behavioral, cholinergic, and toxic effects that were observed. There were no indications of any cholinergic incidental effects, any harmfulness, or no mortality was noticed post organization of test compound BTA 3D. These examinations recommended that compound 3d have a critical wiggle room of security [**22**]

.

Table-2. Animal Grouping for Acute Toxicity

S. No.	Groups	Animal Species	No. of animals
1.	Group 1 (5 mg/kg BW)		3
2.	Group 2 (50 mg/kg BW)	Wistar Rats	3
3.	Group 3 (300 mg/kg BW)		3
4.	Group 4 (2000 mg/kg BW)		3
	Total animals		**12**

Table 2. acute oral toxicity animal grouping by OECD guidelines

Animal Grouping: -

The present study utilized female Wistar rats weighing between 180 and 250 g, and divided them into 6 groups. Group I also served as Normal Control, Group II was the Toxin Control, where rats were administered with scopolamine HBr (0.5mg/kg, *i.p.*) from day 1st to day 28th, and Group III was the (Donepezil 0.5mg/kg *p.o*) + scopolamine HBr (0.5mg/kg, *i.p.*) from day 1st to day 28th. Treatment compound was orally administered to animals in Groups IV, V, and VI at doses of 2mg/kg, 4mg/kg, and 8mg/kg, respectively, from Day 1 to Day 28th. according to standard protocol. Behavioural parameters were assessed on the 0, 1th, 7th, 14th,21th and 28 days. On the 29th day, rats were sacrificed and their brains were immediately preserved at a temperature of -180°C for the estimation of parameters including anti-inflammatory estimation, Biochemical and protein expressions. **(23)**

NOTE: Summarizes the experimental procedure, and a single brain tissue sample from each group was kept in 10% formalin solution for histological examination. The experimental study lasted for a total of 28 days, including 5 days of training period followed by 28 days of experimental study (from day 1st to day 28th).**(24)**

S. No.	Groups / Dose / Treatment	Rats Species	No. of animals
1	Normal Control		06
2	Scopolamine HBr (0.5 mg/kg, *i.p.*) + Vehicle		06
3	Standard - Donepezil (.5 *mg/kg*, *p.o.*) + scopolamine (0.5mg/kg *i.p.*)		06
4	Treatment-1 compound X (2mg/kg, *p.o.*) + scopolamine (0.5mg/kg, *i.p.*)	Wistar Rats	06
5	Treatment-2 compound X (4mg/kg, *p.o.*) + scopolamine (0.5mg/kg, *i.p)*.		06
6	Treatment-3 (8mg/kg, *p.o.*) + scopolamine (0.5mg/kg, *i.p.)*		06
	Total Rats		**36**

Total 3. No. of animals: 36

Y-maze task: The Y-Maze task is the standard creature model utilized for assessment of hippocampal-sub ordinate transient working memory in the rodents. the rate (%) modifications were determined (unconstrained change rate), which showed the functioning memory limit of creatures. The % unconstrained shifts was fundamentally decreased (***$p < 0.001$) in the scopolamine gathering of creatures contrasted with control bunch characteristic of enlistment of memory and learning weakness. Donepezil (.5 mg/kg) and compound BTA 3D showed essentially expanded (###$p < 0.001$) unconstrained shifts contrasted with scopolamine bunch. At the portion of 4 and 8 mg/kg, *p.o.* Comparing compound 3D to donepezil (.5 mg/kg), the percentage of alterations was statistically non-significantly different. The complete arm passages stayed unaltered in all gatherings recommended that scopolamine didn't hamper the locomotor movement in animals(continuously). **(25)**
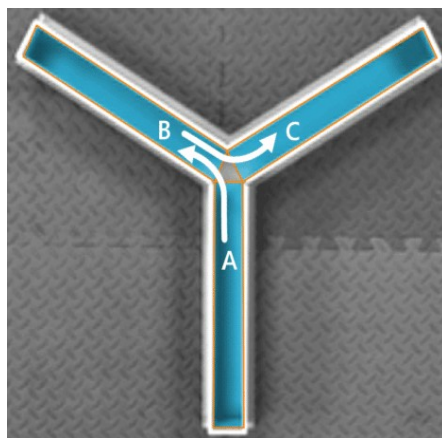
(**Fig.1** Y maze)

Y MAZE TASK RESULTS BY THEIR GROUP DOSE AND SPONTANEOUS ALTERATION

A.
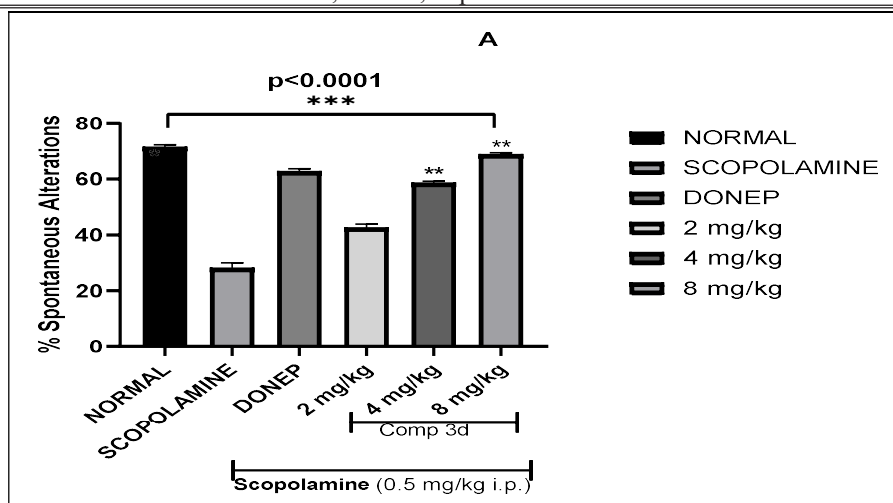
(Fig 2 spontaneous alteration**)**

B.
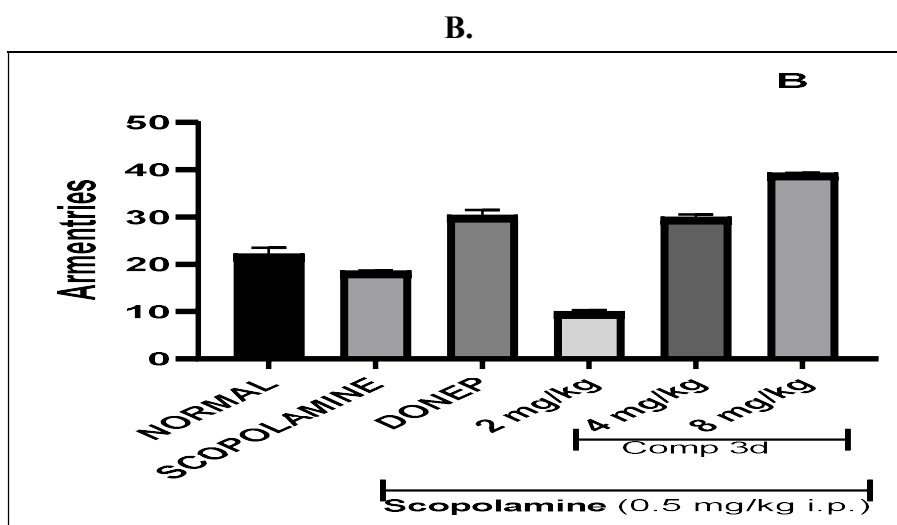
❖   **(Fig 3** arm Entery graph of Rats**)**

Fig. 2,3. (The effects of compound 3D administered topically at doses of 2, 4, and 8 mg/kg donepezil (0.5 mg/kg, orally) by Y-maze test [A] Unconstrained adjustment score (% changes); [B] All out arm sections. All values are addressed as mean $\pm$ SD (n = 6). *** compared to the control, p 0.001; ### p < 0.001 contrasted with scopolamine; ns = non-huge; Done5 = donepezil.) **(26,27)**

DISSECTION AND HOMOGENIZATION

Wister rats were sacrificed via cervical disengagement following diethyl ether deadening once conduct investigations were completed. Immediately, the whole cerebrums were separated and cleaned in cold saline (0.9 percent). To get the homogenates, the whole cerebrum was homogenised in a Teflon-glass homogenizer along with 3 ml of 10 mM cold sodium phosphate

buffer with a final pH of 7.4 and centrifuged at 2-8 °C for 10 min at 11,000 rpm. Additionally, the collected homogenates were used to analyse the various biochemical boundaries. **(28)**

Ex vivo estimation of AChE

The amount of the cholinergic biomarker Throb in the homogenate of the whole brain was determined using the Ellman technique. The method relied on the interaction of the hydrolyzed product of ATCI, thiocholine, and DTNB to produce a yellow-hued substance that could be measured spectrophotometrically at 412 nm. The test mixture, which included 25 ml of tissue homogenate, 150 ml of pH-7.2 0.1 M phosphate support, and 100 ml of 10 mM DTNB, was preincubated for 10 min at room temperature. Expanding 20 l of 75 mM ATCI kicked off the reaction, and absorbance was calculated at 412 nm. Regarding the hydrolyzed substrate, the declaration of ACHE inhibitory strength was taken into consideration. **(29)**

.
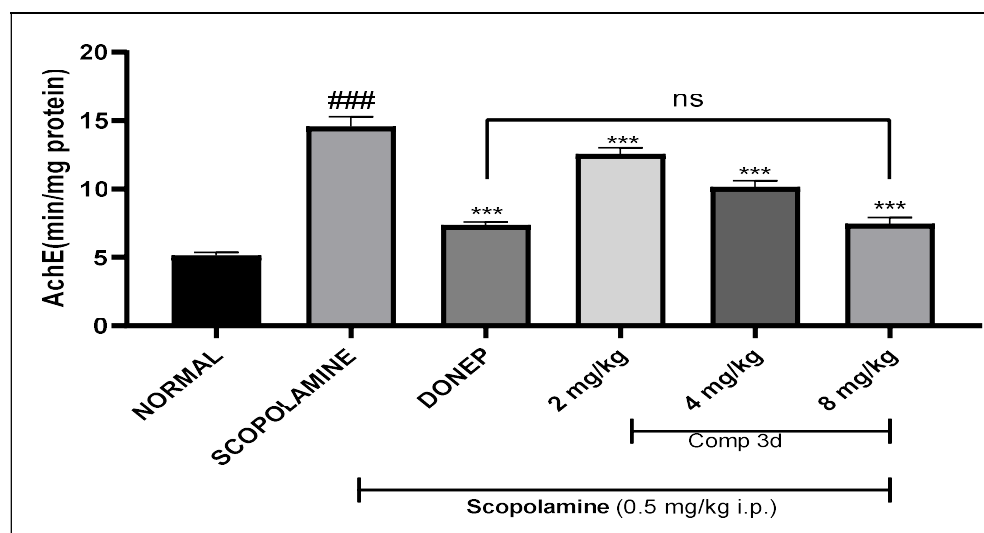
(Fig.4 this figure shows the effect of treatment compound in ache inhibition with significant and non- significant values on different doses) **(30)**

OXIDATIVE STRESS BIOMARKERS ESTIMATIONS

SOD assay

The comprehensive disclosed protocol described by Kono in 1978 allowed for the completion of the Turf examination. The test solution contains 0.1 mM ethylenediamine tetraacetic acid, 96 mM nitro blue tetrazolium, and 50 mM sodium carbonate. The aforesaid mixture (2 ml), 0.05 ml of brain homogenate, and 0.05 ml of hydroxylamine hydrochloride (pH 6.0 maintained by using NaOH) were added to a cuvette, and the adjustment of optical thickness was measured at 560 nm for 2 min at intervals of 30 seconds. **(31)**.
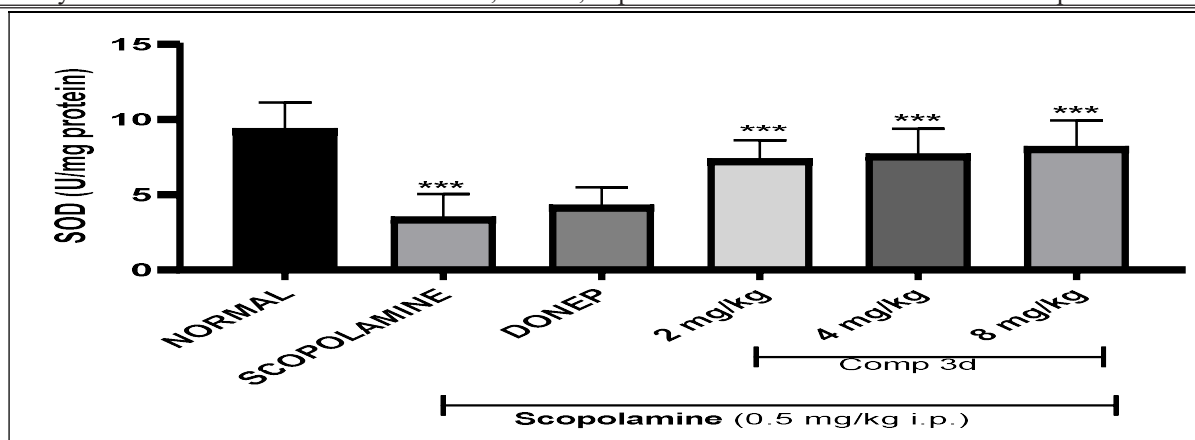
Fig 5 oxidative stress estimation (SOD)

Catalase assay

By combining 1.95 ml of 0.1 M phosphate buffer, pH 7.4, 1 ml of 19 mM H2O2, and 0.05 ml of cerebral homogenate to create a final measure volume of 3.0 ml, the catalase activity examination was carried out. At 240 nm, the absorbance change was assessed, and the results were calculated as mM of catalase activity responsible for the decline in H2O2/min/mg protein. **(32)**
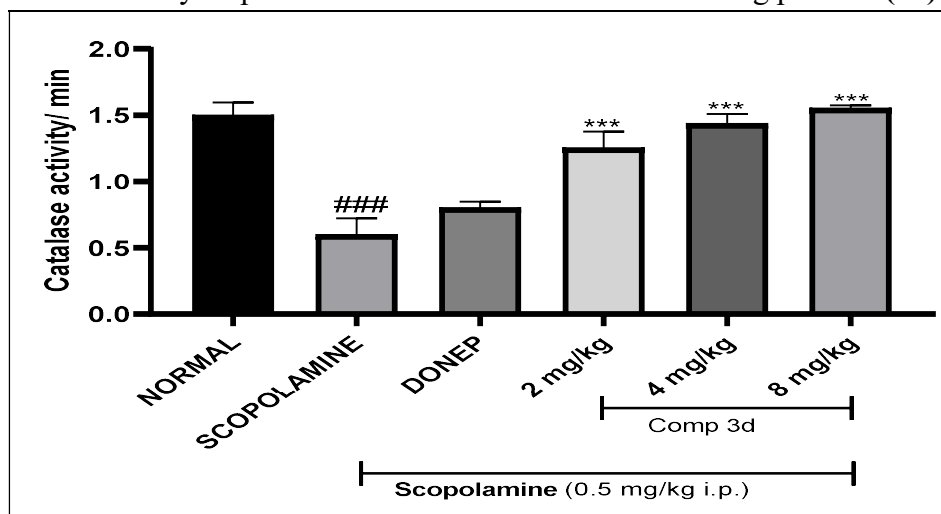
Fig 6. catalase activity estimation on different dosage

HISTOPATHOLOGY

H & E staining (Haematoxylin and Eosin)

The rats were sacrificed at the end of the study, and the brains are isolated then then preserved in 10% formalin (4% formaldehyde), and then set in paraffin wax. Coronal slices of the hippocampus were then cut using a microtome with 5-m thicknesses. The hippocampal slices were dewaxed and then submerged in haematoxylin solution for three minutes. Eosin was then used to stain the slices for an additional 1-2 minutes. The portions were first dehydrated with alcohol before spending 30 seconds submerged in xylene. The hippocampus was marked with haematoxylin and eosin (H &

E), and the damage to the neurons was observable in a light microscope under the magnifications of 4X, 10X, and 40X as described in (Zameer et al., 2021). **(33)**

Results of Histo path lab:

A(normal control)   B (Done. +scop.)   C (scopolamine Hbr)

D [Comp. (2mg/kg)   E   [Comp. (4mg/kg)]   F   [Comp. (8mg/kg)]
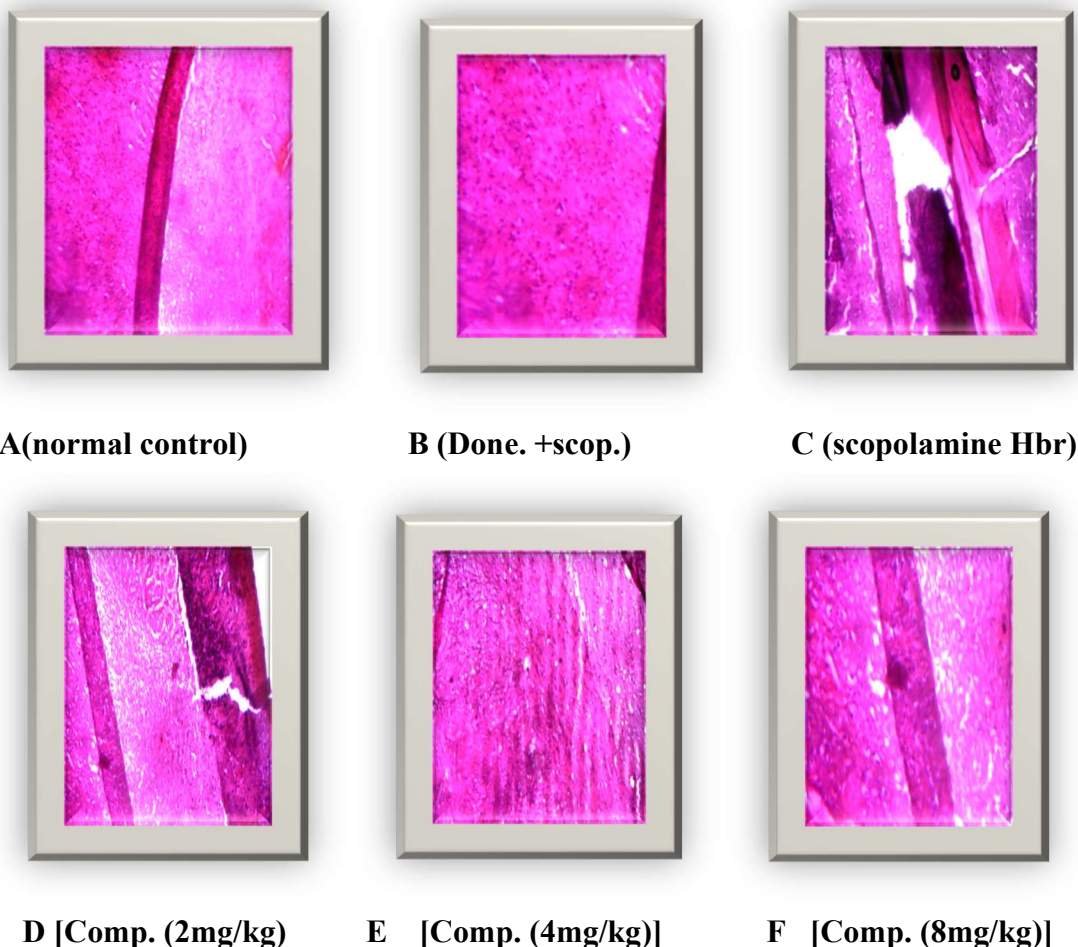
Fig.7 (A – F) *(this figure shows the histo path lab result by different images of different groups that is Comperision between standard drug and synthesized drug by scopolamine induced Alzheimer's group with different compound group (equivalent weight).* **(34)**
Computational Studies

In silico docking simulations:

An in silico molecular docking research for compound BTA 3D was carried out using the Schrödinger Maestro 2018-1 edition on an HP Kernel Linux workstation. The outcomes of the docking investigations were contrasted with donepezil's conventional and co-crystallized forms. The docking investigation used the throb catalyst structure with the co-solidified ligand donepezil from the chemical compound Tetronarce 33 Californica. **(35)**

MOLICULAR DOCKING AND DYNAMICS:

When a ligand and a goal are attached to one another to form a stable complex, a method called docking is used to forecast the preferred direction of one particle to the next. Thus, using scoring capabilities, for example, information on the preferred orientation might be used to predict the degree of connection or restricted like between two particles. **(36,37)**

Ligand information:

No of atoms – 45

Heavy atoms 29

Atomic mass – 404.451

No. of fragments- 4

Num. of rot. Bonds – 8
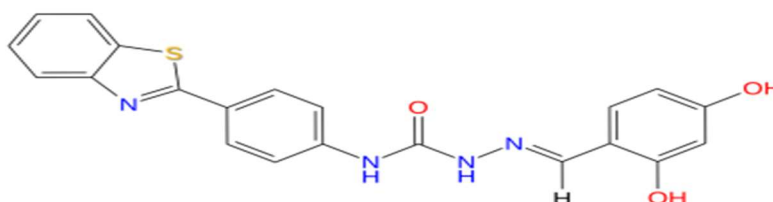
Counter Ion/Salt Information

Type	Num.	Concentration [mM]	Total Charge
Na	55	59.439	+55
Cl	47	50.793	-47
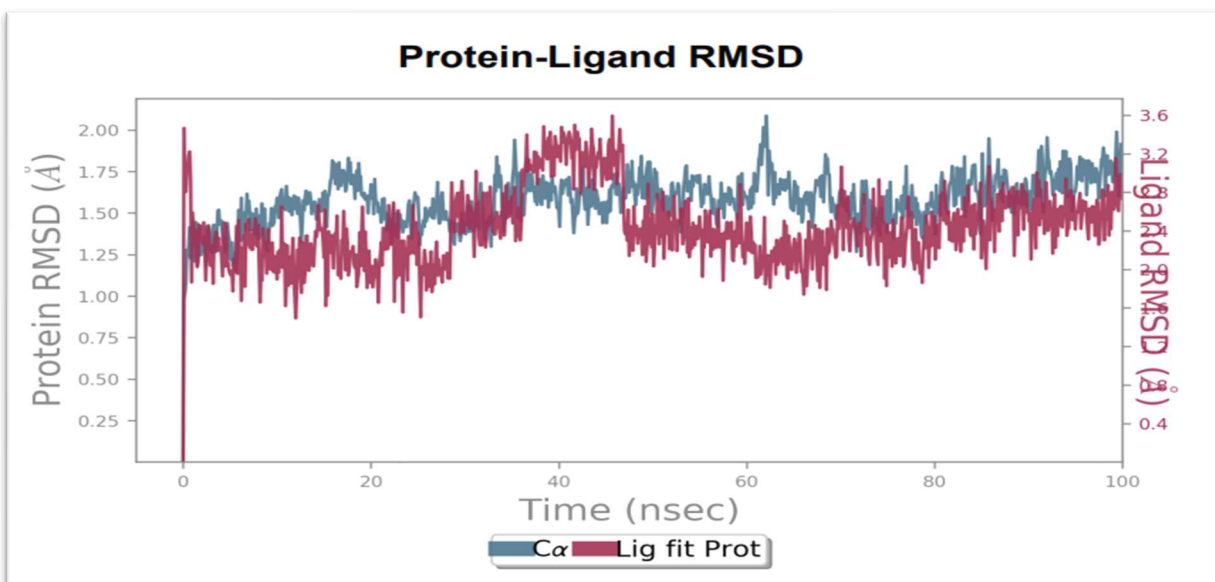
Fig 8. Protein ligand RMSD

The average change in atom displacement for a given frame in relation to a reference frame is measured using the Root Mean Square Deviation (RMSD). It is determined for all edges in the direction. **(38)** The RMSD for outline x is:

$$RMSD_x = \sqrt{\frac{1}{N}\sum_{i=1}^{N}(r_i'(t_x)) - r_i(t_{ref}))^2}$$

N is the number of atoms in the selected molecule, and t ref is the reference time (typically, the leading edge is used as the reference and is considered to be time t=0). Additionally, the position of the chosen particles in outline x after superimposing on the reference outline, where outline x is recorded at time t x, is indicated by the symbol r'. The procedure is repeated in the reverse direction for each casing**. (39)**

Protein RMSF:
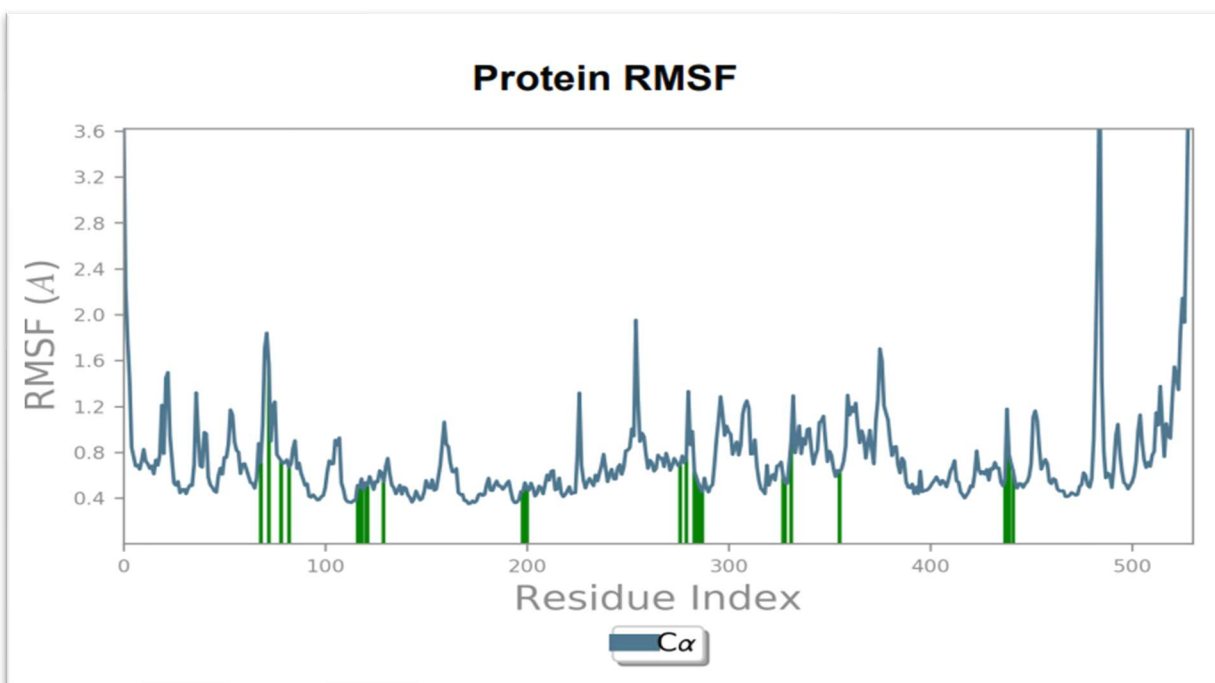
Fig. 9 protein RMSF

The Root Mean Square Vacillation (RMSF) is valuable for describing nearby changes along the protein chain. The RMSF for buildup I is:

$$RMSF_i = \sqrt{\frac{1}{T} \sum_{t=1}^{T} < (r_i'(t)) - r_i(t_{ref}))^2 >}$$

where T denotes the trajectory time used to calculate the RMSF, t ref denotes the reference time, r I denotes the position of residue I r' denotes the position of atoms in residue I after superposition on the reference, and the angle brackets denote that the square distance is averaged over a subset of atoms in the residue. Peaks on this map represent regions of the protein that vary most during the simulation. Usually, you'll notice that the protein's N- and C-terminal tails move more than any other area. Typically more rigid than the protein's unstructured portion, secondary structural components like alpha helices and beta strands change less than loop sections. **(40)**

Ligand Contacts: Green vertical bars indicate protein residues that interact with the ligand. **(41)**

PROTEIN SECONDARY SRUCTURE –

Fig 10. Protein secondary structure with residue index

Protein optional design components (SSE) like alpha-helices and beta-strands are observed all through the reenactment. The SSE spreading by residue index throughout the protein structure is depicted in the graph above. The plot underneath sums up the SSE organization for every direction outline throughout the span of the reproduction, and the plot at the base screens every buildup and its SSE task over the long run.
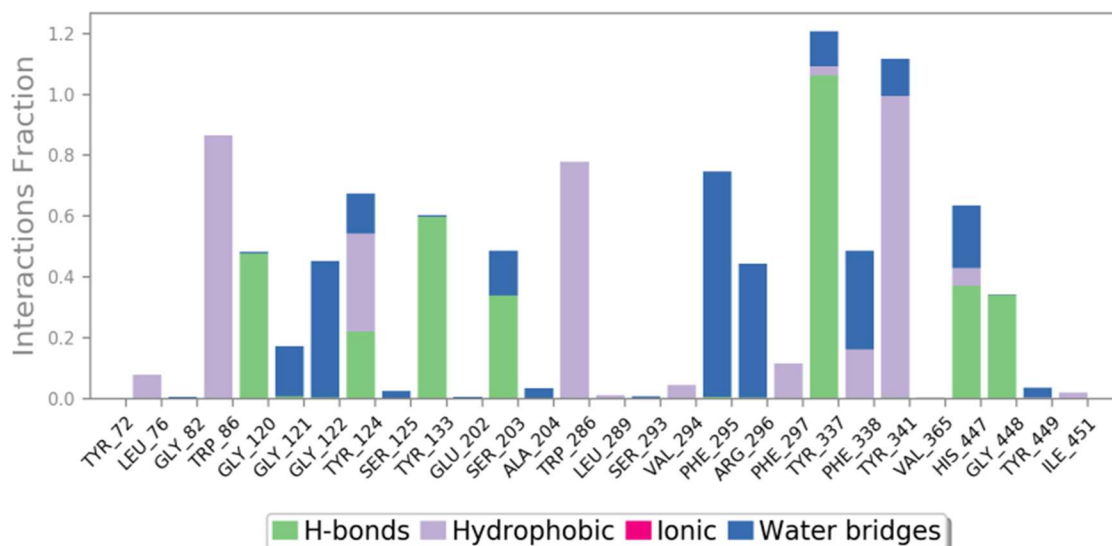
Fig 11. Protein ligand binding

Protein associations with the ligand can be observed all through the reproduction. These communications can be sorted by type and summed up, as displayed in the plot above. There are four kinds of "contacts" between proteins and ligands: Hydrogen Bonds, Hydrophobic, Ionic and Water Extensions. The "Simulation Interactions Diagram" panel lets you look into more specific subtypes of each interaction type. The stacked bar graphs are standardized throughout the span of the direction: for instance, a worth of 0.7 proposes that 70% of the recreation time the particular collaboration is kept up with. Values over 1.0 are conceivable as some protein buildup might make different contacts of same subtype with the ligand**. (42)**

Hydrogen Bonds: (H-bonds) assume a critical part in ligand restricting. Thought of hydrogen-holding properties in drug configuration is significant as a result of areas of strength for them on drug particularity, utilization and adsorption. Hydrogen connections between a protein and a ligand can be additionally separated into four subtypes: spine acceptor; donor of the bone; acceptor on the sidechain; side-chain benefactor. The following are the current geometric criteria for the protein-ligand H-bond: distance of 2.5 Å between the giver and acceptor particles (D — H···A); a contributor point of ≥120° between the giver hydrogen-acceptor particles (D — H···A); also, an acceptor point of ≥90° between the hydrogen-acceptor-bonded_atom as (H···A — X). **(43)**

Hydrophobic contacts: have three subtypes: π-Cation; π-π; also, Other, vague communications. By and large these sort of communications include a hydrophobic amino corrosive and a sweet-smelling or aliphatic gathering on the ligand, however we have stretched out this classification to likewise incorporate π-Cation cooperations. The ongoing mathematical rules for hydrophobic cooperations is as per the following: π-Cation — Fragrant and charged bunches inside 4.5 Å; - consists of two aromatic groups stacked side by side or edge to edge; Other. A hydrophobic

sidechain that is not specific and is located within 3.6 of the aromatic or aliphatic carbons of a ligand.**(44)**

Ionic interactions: Particle interaction or polar communications, are between two oppositely charged molecules that are inside 3.7 Å of one another and don't include a hydrogen security. We likewise screen Protein-Metal-Ligand communications, which are characterized by a metal particle composed inside 3.4 Å of protein's and ligand's weighty iotas (with the exception of carbon). All ionic cooperations are separated into two subtypes: those intervened by a protein spine or side chains. Floating Bridges: are hydrogen-reinforced protein-ligand communications interceded by a water particle. The hydrogen-bond math is somewhat loose from the standard H-bond definition. The following are the current geometric requirements for a protein-water or water-ligand H-bond: the donor and acceptor atoms are separated by 2.8 (D—H—A); a benefactor point of ≥110° between the contributor hydrogen-acceptor molecules (D — H⋯A); also, an acceptor point of ≥90° between the hydrogen-acceptor-bonded_atom particles (H⋯A — X).(**45**)
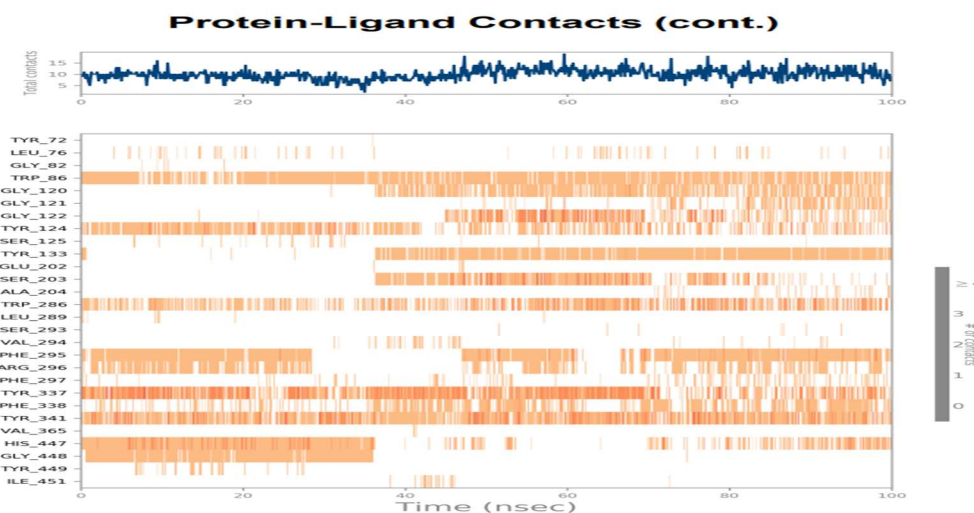
Fig.12 (ionic interactions and contacts (H-bonds, Hydrophobic, Ionic, Water bridges)

A timetable representation of the contacts and interactions (H-bonds, Hydrophobic, Ionic, Water spans) summed up in the past page. **(46)** The top board shows the absolute number of explicit associates the protein makes with the ligand throughout the span of the direction. The base board shows which deposits communicate with the ligand in every direction outline. A few buildups make more than one explicit contact with the ligand, which is addressed by a hazier shade of orange, as per the measure to one side of the plot. **(47)**

Fig.13 Ligand-protein contacts
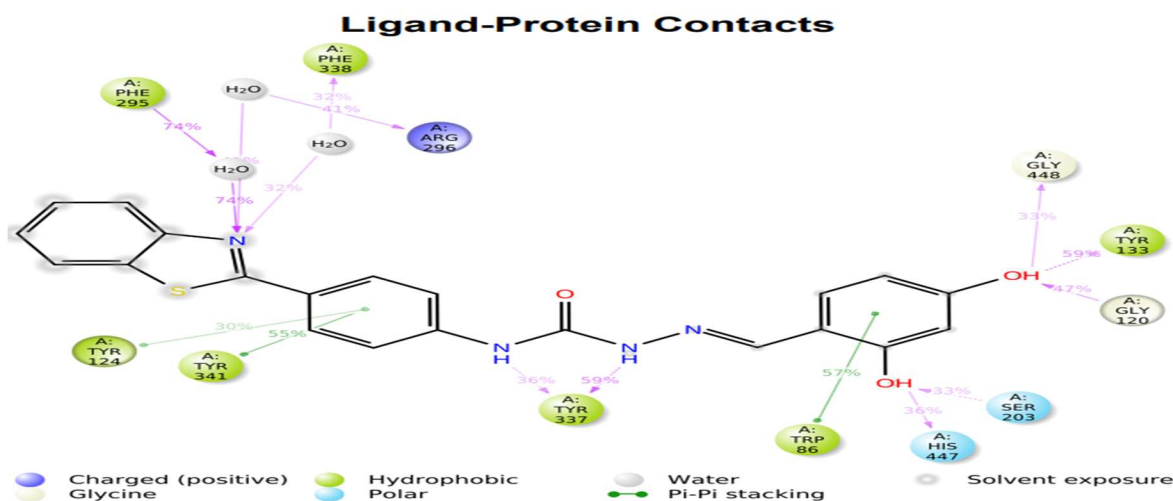
A schematic of detailed ligand atom interactions with the protein residues. Interactions that occur more than 30.0% of the simulation time in the selected trajectory (0.00 through 100.00 nsec), are shown. **(48)** As a result, the hydrophobic and pi-pi stacking properties of bta 3d in this ligand protein binding.

Note: Because some remains may have multiple communications of the same type with the same ligand atom, it is possible to have interactions with more than 100%. For instance, the ARG side chain has four H-bond contributors that can all hydrogen-cling to a solitary H-bond acceptor. **(49)**

CONCLUSION:

The FDA-approved AChE inhibitors that are now available can only offer symptomatic alleviation to AD patients. The primary objective for medicinal chemists continues to be the quest for a fresh lead for the treatment of AD, despite the fact that this effort has long been unsuccessful. A fresh batch of benzothiazole compounds were created, manufactured, and studied using spectroscopic methods in our search for a brand-new lead (FT-IR, 1H NMR, and 13C NMR). All the results were in agreement with the structures of the synthesized compounds. The created and produced analogues demonstrated compound BTA 3D's suppression of AChE. Additionally, compound BTA 3D demonstrated good AChE inhibitory activity. Additionally, three dosages of the most effective molecule, BTA 3D, were used in rat Y-maze tests to examine in vivo behavioural research. The results indicated that compound BTA 3D improved learning and memory in a dosage-dependent manner, with the largest impact being shown at the dose of 8 mg/kg, orally. Ex vivo experiments and biochemical analysis were also carried out, which demonstrated the compound BTA 3D's potent AChE inhibition and antioxidant properties, respectively. Consensual binding interactions of compound BTA 3D with AChE's catalytic and peripheral anionic site residues were found in in silico molecular docking and dynamics investigations. The potential of compound BTA 3D to be developed as the key ingredient in the creation of orally active therapies for the treatment of AD was underlined by all of these findings.

REFERENCES

1   Breijyeh, Zeinab, and Rafik Karaman. "Comprehensive review on Alzheimer's disease: Causes and treatment." *Molecules* 25, no. 24 (2020): 5789.

2   Tayeb, Haythum O., Hyun Duk Yang, Bruce H. Price, and Frank I. Tarazi. "Pharmacotherapies for Alzheimer's disease: beyond cholinesterase inhibitors." *Pharmacology & therapeutics* 134, no. 1 (2012): 8-25.

3   Dantzer, Robert, Jason C. O'connor, Gregory G. Freund, Rodney W. Johnson, and Keith W. Kelley. "From inflammation to sickness and depression: when the immune system subjugates the brain." *Nature reviews neuroscience* 9, no. 1 (2008): 46-56.

4   Alzheimer's disease: an hypothesis, Trends Neurosci., 10 (1987) 65-68

5   Oliveri, Valentina, and Graziella Vecchio. "8-Hydroxyquinolines in medicinal chemistry: A structural perspective." *European journal of medicinal chemistry* 120 (2016): 252-274.

6   Xie, Jiayang, Ruirui Liang, Yajiang Wang, Junyi Huang, Xin Cao, and Bing Niu. "Progress in target drug molecules for Alzheimer's disease." *Current Topics in Medicinal Chemistry* 20, no. 1 (2020): 4-36.

7   Bull, James A., Rosemary A. Croft, Owen A. Davis, Robert Doran, and Kate F. Morgan. "Oxetanes: recent advances in synthesis, reactivity, and medicinal chemistry." *Chemical Reviews* 116, no. 19 (2016): 12150-12233.

8   Wahlgren, Curtis G., Anthony W. Addison, Sudhir Burman, Laurence K. Thompson, Ekkehard Sinn, and Theresa M. Rowe. "Oxo-bridged complexes of iron (III) derived from 2-(2′-hydroxyphenyl)-benzothiazole and 2-(2′-hydroxyphenyl) benzimidazole ligands." *Inorganica chimica acta* 166, no. 1 (1989): 59-69.

9   Musatat, Ahmad Badreddin, Alparslan Atahan, Adem Ergün, Kübra Çıkrıkcı, Nahit Gençer, Oktay Arslan, and Mustafa Zengin. "Synthesis, enzyme inhibition, and molecular docking studies of a novel chalcone series bearing benzothiazole scaffold." *Biotechnology and Applied Biochemistry* 70, no. 3 (2023): 1357-1370.

10   Jeffries, Daniel E. *Discoveries and Challenges Encountered Towards the Development of a Metabotropic Glutamate Receptor 3 Positive Allosteric Modulator. Synthesis and Biological Evaluation of Hybrubin A. Synthesis of Natural and Unnatural Dibenzylbutane Lignans from a Shared Intermediate*. Vanderbilt University, 2019.

11   Ghannam, Iman AY, Eman A. Abd El-Meguid, Islam H. Ali, Donia H. Sheir, and Ahmed M. El Kerdawy. "Novel 2-arylbenzothiazole DNA gyrase inhibitors: Synthesis, antimicrobial evaluation, QSAR and molecular docking studies." *Bioorganic Chemistry* 93 (2019): 103373.

12   Pan, Ying-Qi, Meng Yu, Yu Zhang, and Wen-Kui Dong. "Synthesis and crystal structure of (1 E, 3 E)-2-hydroxy-5-methylisophthalaldehyde O, O-di (2-((((E)-(2-hydroxynaphthalen-1-yl) methylene) amino) oxy) ethyl) dioxime, C35H32N4O7." *Zeitschrift für Kristallographie-New Crystal Structures* 235, no. 2 (2020): 429-431.

13   Uma, P., K. C. Rajanna, Y. Hemanth Sriram, and P. K. Saiprakash. "a facile synthesis of 2-(4-(benzo [d] thiazol-2-yl) phenylimino) thiazolidin-4-one and 2-(4-(benzo [d] thiazol-2-yl) phenylimino)-5-arylidenethiazolidin-4-ones." *Rasayan Journal of Chemistry* 10, no. 2 (2017).

14   Samala, Ganesh, Chunduri Madhuri, Jonnalagadda Padma Sridevi, Radhika Nallangi, Yogeeswari Perumal, and Sriram Dharmarajan. "Synthesis and antitubercular evaluation of 2-iminothiazolidine-4-ones." *European Journal of Chemistry* 5, no. 3 (2014): 550-556.

15   Ghorbanloo, Massomeh, Rahman Bikas, and Grzegorz Małecki. "New molybdenum (VI) complexes with thiazole-hydrazone ligand: preparation, structural characterization, and catalytic applications in olefin epoxidation." *Inorganica Chimica Acta* 445 (2016): 8-16.

16   Mishchenko, Mariia, Sergiy Shtrygol, Danylo Kaminskyy, and Roman Lesyk. "Thiazole-bearing 4-thiazolidinones as new anticonvulsant agents." *Scientia Pharmaceutica* 88, no. 1 (2020): 16.

17   Nastasă, Cristina, Brîndușa Tiperciuc, Mihaela Duma, Daniela Benedec, and Ovidiu Oniga. "New hydrazones bearing thiazole scaffold: Synthesis, characterization, antimicrobial, and antioxidant investigation." *Molecules* 20, no. 9 (2015): 17325-17338.

18   Abdel-Wahab, Bakr F., Salwa F. Mohamed, Abd El-Galil E. Amr, and Mohamed M. Abdalla. "Synthesis and reactions of thiosemicarbazides, triazoles, and Schiff bases as antihypertensive α-blocking agents." *Monatshefte für Chemie-Chemical Monthly* 139 (2008): 1083-1090.

19   Pancholia, Sahaj, Tejas M. Dhameliya, Parth Shah, Pradeep S. Jadhavar, Jonnalagadda Padma Sridevi, Perumal Yogeshwari, Dharmarajan Sriram, and Asit K. Chakraborti. "Benzo [d] thiazol-2-yl (piperazin-1-yl) methanones as new anti-mycobacterial chemotypes: Design, synthesis, biological evaluation and 3D-QSAR studies." *European Journal of Medicinal Chemistry* 116 (2016): 187-199.

20   Crumbaugh, James C., and Leonard T. Maholick. "An experimental study in existentialism: The psychometric approach to Frankl's concept of noogenic neurosis." *Journal of clinical psychology* 20, no. 2 (1964): 200-207.

21   Fisher, Bonnie S. "The effects of survey question wording on rape estimates: Evidence from a quasi-experimental design." *Violence against women* 15, no. 2 (2009): 133-147.

22   Chauhdary, Zunera, Uzma Saleem, Bashir Ahmad, Shahid Shah, and Muhammad Ajmal Shah. "Neuroprotective evaluation of Tribulus terrestris L. In aluminum chloride induced Alzheimer's disease." *Pakistan journal of pharmaceutical sciences* 32 (2019).

23 Dhami, Mahadev, Khadga Raj, and Shamsher Singh. "Neuroprotective effect of fucoxanthin against intracerebroventricular streptozotocin (ICV-STZ) induced cognitive impairment in experimental rats." *Current Alzheimer Research* 18, no. 8 (2021): 623-637.

24 Ohta, H., H. Nishikawa, H. Kimura, H. Anayama, and M. Miyamoto. "Chronic cerebral hypoperfusion by permanent internal carotid ligation produces learning impairment without brain damage in rats." *Neuroscience* 79, no. 4 (1997): 1039-1050.

25 Tournier, Benjamin B., Cristina Barca, Aïda B. Fall, Yesica Gloria, Léa Meyer, Kelly Ceyzériat, and Philippe Millet. "Spatial reference learning deficits in absence of dysfunctional working memory in the tgf344-AD rat model of Alzheimer's disease." *Genes, Brain and Behavior* 20, no. 5 (2021): e12712.

26 Mishra, Puja, Piyoosh Sharma, Prabhash Nath Tripathi, Sukesh Kumar Gupta, Pavan Srivastava, Ankit Seth, Avanish Tripathi, Sairam Krishnamurthy, and Sushant Kumar Shrivastava. "Design and development of 1, 3, 4-oxadiazole derivatives as potential inhibitors of acetylcholinesterase to ameliorate scopolamine-induced cognitive dysfunctions." *Bioorganic Chemistry* 89 (2019): 103025.

27 Tripathi, Prabhash Nath, Pavan Srivastava, Piyoosh Sharma, Manish Kumar Tripathi, Ankit Seth, Avanish Tripathi, Sachchida Nand Rai, Surya Pratap Singh, and Sushant K. Shrivastava. "Biphenyl-3-oxo-1, 2, 4-triazine linked piperazine derivatives as potential cholinesterase inhibitors with anti-oxidant property to improve the learning and memory." *Bioorganic Chemistry* 85 (2019): 82-96.

28 Underwood, Wendy, Raymond Anthony, S. Cartner, D. Corey, T. Grandin, C. Greenacre, S. Gwaltney-Brant, M. A. Mccrackin, R. Meyer, and D. Miller. "AVMA guidelines for the euthanasia of animals: 2013 edition." Schaumburg, IL: American Veterinary Medical Association, 2013.

29 Srivastava, Pavan, Prabhash Nath Tripathi, Piyoosh Sharma, and Sushant Kumar Shrivastava. "Design, synthesis, and evaluation of novel N-(4-phenoxybenzyl) aniline derivatives targeting acetylcholinesterase, β-amyloid aggregation and oxidative stress to treat Alzheimer's disease." *Bioorganic & Medicinal Chemistry* 27, no. 16 (2019): 3650-3662.

30 Ahmed, Touqeer, and Anwarul-Hassan Gilani. "Inhibitory effect of curcuminoids on acetylcholinesterase activity and attenuation of scopolamine-induced amnesia may explain medicinal use of turmeric in Alzheimer's disease." *Pharmacology Biochemistry and Behavior* 91, no. 4 (2009): 554-559.

31 Mishra, Puja, Piyoosh Sharma, Prabhash Nath Tripathi, Sukesh Kumar Gupta, Pavan Srivastava, Ankit Seth, Avanish Tripathi, Sairam Krishnamurthy, and Sushant Kumar Shrivastava. "Design and development of 1, 3, 4-oxadiazole derivatives as potential inhibitors of acetylcholinesterase to ameliorate scopolamine-induced cognitive dysfunctions." *Bioorganic Chemistry* 89 (2019): 103025.

32 Kumar, Baldeep, Anurag Kuhad, and Kanwaljit Chopra. "Neuropsychopharmacological effect of sesamol in unpredictable chronic mild stress model of depression: behavioral and biochemical evidences." *Psychopharmacology* 214 (2011): 819-828.

33　Shahid, Farah, Aneela Zameer, and Muhammad Muneeb. "A novel genetic LSTM model for wind power forecast." *Energy* 223 (2021): 120069.

34　Mishra, Puja, Piyoosh Sharma, Prabhash Nath Tripathi, Sukesh Kumar Gupta, Pavan Srivastava, Ankit Seth, Avanish Tripathi, Sairam Krishnamurthy, and Sushant Kumar Shrivastava. "Design and development of 1, 3, 4-oxadiazole derivatives as potential inhibitors of acetylcholinesterase to ameliorate scopolamine-induced cognitive dysfunctions." *Bioorganic Chemistry* 89 (2019): 103025.

35　Kaur, Tejinder, Ashwini Madgulkar, Mangesh Bhalekar, and Kalyani Asgaonkar. "Molecular docking in formulation and development." *Current Drug Discovery Technologies* 16, no. 1 (2019): 30-39.

36　Alonso, Hernan, Andrey A. Bliznyuk, and Jill E. Gready. "Combining docking and molecular dynamic simulations in drug design." *Medicinal research reviews* 26, no. 5 (2006): 531-568.

37　Roe, Daniel R., and Thomas E. Cheatham III. "PTRAJ and CPPTRAJ: software for processing and analysis of molecular dynamics trajectory data." *Journal of chemical theory and computation* 9, no. 7 (2013): 3084-3095.

38　Paul, Parag Kumar, Salauddin Al Azad, Mohammad Habibur Rahman, Mithila Farjana, Muhammad Ramiz Uddin, Dipta Dey, Shafi Mahmud et al. "Catabolic profiling of selective enzymes in the saccharification of non-food lignocellulose parts of biomass into functional edible sugars and bioenergy: An in silico bioprospecting." *Journal of advanced veterinary and animal research* 9, no. 1 (2022): 19.

39　Patel, Preeti, Sushant Kumar Shrivastava, Piyoosh Sharma, Balak Das Kurmi, Ekta Shirbhate, and Harish Rajak. "Hydroxamic acid derivatives as selective HDAC3 inhibitors: computer-aided drug design strategies." *Journal of Biomolecular Structure and Dynamics* (2023): 1-22.

40　Harikrishna, A. S., and Kesavan Venkitasamy. "Identification of novel human nicotinamide N-methyltransferase inhibitors: a structure-based pharmacophore modeling and molecular dynamics approach." *Journal of Biomolecular Structure and Dynamics* (2023): 1-13.

41　Daood, Umer, Jukka P. Matinlinna, Malikarjuna Rao Pichika, Kit-Kay Mak, Venkateshbabu Nagendrababu, and Amr S. Fawzy. "A quaternary ammonium silane antimicrobial triggers bacterial membrane and biofilm destruction." *Scientific reports* 10, no. 1 (2020): 10970.

42　Schaller, David, Dora Šribar, Theresa Noonan, Lihua Deng, Trung Ngoc Nguyen, Szymon Pach, David Machalz, Marcel Bermudez, and Gerhard Wolber. "Next generation 3D pharmacophore modeling." *Wiley Interdisciplinary Reviews: Computational Molecular Science* 10, no. 4 (2020): e1468.

43　Hernandes, Marcelo Z., Suellen Melo T. Cavalcanti, Diogo Rodrigo M. Moreira, Walter Filgueira de Azevedo Junior, and Ana Cristina Lima Leite. "Halogen atoms in the modern medicinal chemistry: hints for the drug design." *Current drug targets* 11, no. 3 (2010): 303-314.

44　Sangai, Neha P., Chirag N. Patel, and Himanshu A. Pandya. "Ameliorative effects of quercetin against bisphenol A-caused oxidative stress in human erythrocytes: an in vitro and in silico study." *Toxicology research* 7, no. 6 (2018): 1091-1099.

45 Czaja, Kornelia, Jacek Kujawski, Paweł Śliwa, Rafał Kurczab, Radosław Kujawski, Anna Stodolna, Agnieszka Myślińska, and Marek K. Bernard. "Theoretical investigations on interactions of arylsulphonyl indazole derivatives as potential ligands of VEGFR2 kinase." *International Journal of Molecular Sciences* 21, no. 13 (2020): 4793.

46 Allegra, Mario, Marco Tutone, Luisa Tesoriere, Alessandro Attanzio, Giulia Culletta, and Anna Maria Almerico. "Evaluation of the ikkβ binding of indicaxanthin by induced-fit docking, binding pose metadynamics, and molecular dynamics." *Frontiers in Pharmacology* 12 (2021): 701568.

47 Cai, Zhi, Guoyin Zhang, Bin Tang, Yan Liu, Xiaojing Fu, and Xuejin Zhang. "Promising anti-influenza properties of active constituent of Withania somnifera ayurvedic herb in targeting neuraminidase of H1N1 influenza: computational study." *Cell biochemistry and biophysics* 72 (2015): 727-739.

48 Noor, Hasnat, Ayesha Ikram, Thirumalaisamy Rathinavel, Suresh Kumarasamy, Muhammad Nasir Iqbal, and Zohaib Bashir. "Immunomodulatory and anti-cytokine therapeutic potential of curcumin and its derivatives for treating COVID-19–a computational modeling." *Journal of Biomolecular Structure and Dynamics* 40, no. 13 (2022): 5769-5784.

49 Mcdonald, I.K. and Thornton, J.M., 1994. Satisfying hydrogen bonding potential in proteins. *Journal of molecular biology*, *238*(5), pp.777-793.